nature biotechnology

Improved monomeric red, orange and yellow fluorescent proteins derived from *Discosoma* sp. red fluorescent protein

Nathan C Shaner[1], Robert E Campbell[1,6], Paul A Steinbach[1], Ben N G Giepmans[3,4], Amy E Palmer[1] & Roger Y Tsien[1,2,5]

Fluorescent proteins are genetically encoded, easily imaged reporters crucial in biology and biotechnology[1,2]. When a protein is tagged by fusion to a fluorescent protein, interactions between fluorescent proteins can undesirably disturb targeting or function[3]. Unfortunately, all wild-type yellow-to-red fluorescent proteins reported so far are obligately tetrameric and often toxic or disruptive[4,5]. The first true monomer was mRFP1, derived from the *Discosoma* sp. fluorescent protein "DsRed" by directed evolution first to increase the speed of maturation[6], then to break each subunit interface while restoring fluorescence, which cumulatively required 33 substitutions[7]. Although mRFP1 has already proven widely useful, several properties could bear improvement and more colors would be welcome. We report the next generation of monomers. The latest red version matures more completely, is more tolerant of N-terminal fusions and is over tenfold more photostable than mRFP1. Three monomers with distinguishable hues from yellow-orange to red-orange have higher quantum efficiencies.

Although mRFP1 overcame DsRed's tetramerization and sluggish maturation and exceeded DsRed's excitation and emission wavelengths by about 25 nm, the extinction coefficient, fluorescence quantum yield and photostability decreased somewhat during its evolution[7]. To minimize these sacrifices, we subjected mRFP1 to many rounds of directed evolution using both manual and fluorescence-activated cell sorting (FACS)-based screening. The properties of the resulting variants include several new colors, increased tolerance of N- and C-terminal fusions, and improvements in extinction coefficients, quantum yields and photostability, although no single variant is optimal by all criteria.

The red chromophore of DsRed results from the autonomous multi-step post-translational modification of residues Gln66, Tyr67 and Gly68 into an imidazolidinone heterocycle with *p*-hydroxybenzylidene and acylimine substituents[8]. Our first attempt at improving the brightness of mRFP1 involved construction of a directed library in which residues near the chromophore, including position 66, were randomized. The top clone of this library, mRFP1.1, contains the mutation Q66M, which promotes more complete maturation and provides an additional 5 nm red-shift of both the excitation and emission spectra relative to mRFP1. We then set out to reduce the sensitivity of mRFP1.1 to N-terminal fusions. Because *Aequorea victoria* green fluorescent protein (GFP) is relatively indifferent to N- or C-terminal fusions, we eventually generated mRFP1.3 by replacing the first seven amino acids of mRFP1.1 with the corresponding residues from enhanced GFP (MVSKGEE) followed by a spacer sequence NNMA (numbered 6a–d), and appending the last seven amino acids of GFP to the C terminus. mRFP1.3, unlike its predecessors, was found to have an equivalent high level of fluorescence regardless of fusions to its N terminus.

Through additional rounds of screening random libraries based on mRFP1.3 and wavelength-shifted mRFP variants, we identified the beneficial folding mutations V7I and M182K, which were incorporated into clone mRFP1.4. Randomization of position 163 in mRFP1.4 led to the identification of the substitution M163Q, which results in a nearly complete disappearance of the absorbance peak at ~510 nm, present in all previous mRFP clones. The additional mutations N6aD, R17H, K194N, T195V and D196N were introduced through two further rounds of directed evolution to produce our final optimized clone, mCherry (**Table 1** and **Figs. 1**, **2** and **3**).

To test whether the introduction of GFP-type termini into mRFP variants would benefit fusion proteins expressed in mammalian cells, we fused mRFP1 and mCherry to the N terminus of α-tubulin. In most HeLa cells, expression of mRFP1-α-tubulin resulted in diffuse cytoplasmic fluorescence rather than proper incorporation into microtubules (**Fig. 3b**). However, mCherry-α-tubulin fusions were successfully incorporated into microtubules in most cells (**Fig. 3c**), similar to results seen with GFP-coupled tubulin[9]. The amount of full-length mRFP1-α-tubulin expressed was similar to that of mCherry-α-tubulin as verified by in-gel fluorescence and western blot analysis (data not shown). Equivalent results were obtained with Madin-Darby canine kidney and primary human fibroblasts (data not shown). By

[1]Departments of Pharmacology, [2]Chemistry and Biochemistry, and [3]Neurosciences, [4]National Center of Microscopy and Imaging Research, and [5]Howard Hughes Medical Institute, University of California at San Diego, 9500 Gilman Drive, La Jolla, California 92093, USA. [6]Present address: Department of Chemistry, University of Alberta, Edmonton, Alberta T6G 2G2, Canada. Correspondence should be addressed to (rtsien@ucsd.edu).

Published online 21 November 2004; doi:10.1038/nbt1037

Table 1 Properties of novel fluorescent protein variants

Fluorescent protein	Excitation maximum (nm)	Emission maximum (nm)	Extinction coefficient per chain[a] ($M^{-1}cm^{-1}$)	Fluorescence quantum yield	Brightness of fully mature protein (% of DsRed)	pKa	$t_{0.5}$ for maturation at 37 °C	$t_{0.5}$ for bleach[b], s
DsRed	558	583	75,000	0.79	100	4.7	~10 h	ND
T1	555	584	38,000	0.51	33	4.8	<1 h	ND
Dimer2	552	579	69,000	0.69	80	4.9	~2 h	ND
mRFP1	584	607	50,000	0.25	21	4.5	<1 h	6.2
mHoneydew	487/504	537/562	17,000	0.12	3	<4.0	ND	5.9
mBanana	540	553	6,000	0.70	7	6.7	1 h	1.4
mOrange	548	562	71,000	0.69	83	6.5	2.5 h	6.4
dTomato	554	581	69,000	0.69	80	4.7	1 h	64
tdTomato	554	581	138,000	0.69	160	4.7	1 h	70
mTangerine	568	585	38,000	0.30	19	5.7	ND	5.1
mStrawberry	574	596	90,000	0.29	44	<4.5	50 min	11
mCherry	587	610	72,000	0.22	27	<4.5	15 min	68

[a]Extinction coefficients were measured by the alkali denaturation method[8,30] and are believed to be more accurate than the previously reported values for DsRed, T1, dimer2 and mRFP1[7]. [b]Time (s) to bleach to 50% emission intensity, at an illumination level that causes each molecule to emit 1,000 photons/s initially, that is, before any bleaching has occurred. See Methods for more details. For comparison, the value for EGFP is 115 s, assuming an extinction coefficient of 56,000 $M^{-1}cm^{-1}$ and quantum efficiency of 0.60 (ref. 30). ND, not determined.

contrast, fusions of β-actin with mRFP1 or mCherry were both successfully incorporated into the actin cytoskeleton (data not shown).

The dimer2 variant previously described[7] possesses many desirable properties, such as a faster and more complete maturation than wild-type DsRed and a greater fluorescent brightness than the fast-maturing mutant T1 (ref. 6) (DsRed-Express). Through five rounds of directed evolution, we found the optimal combination of mutations to be V22M, Q66M, V105L and F124M, which resulted in improved maturation kinetics, a substantially reduced 'dead-end' green component and a small red-shift. The final clone, designated dimer (d)Tomato (**Table 1** and **Figs. 1** and **2b**), contains GFP-type termini similar to those of mCherry, which result in a higher tolerance of N- and C-terminal fusions (data not shown). To construct a non-aggregating tag from the extremely bright dTomato, we genetically

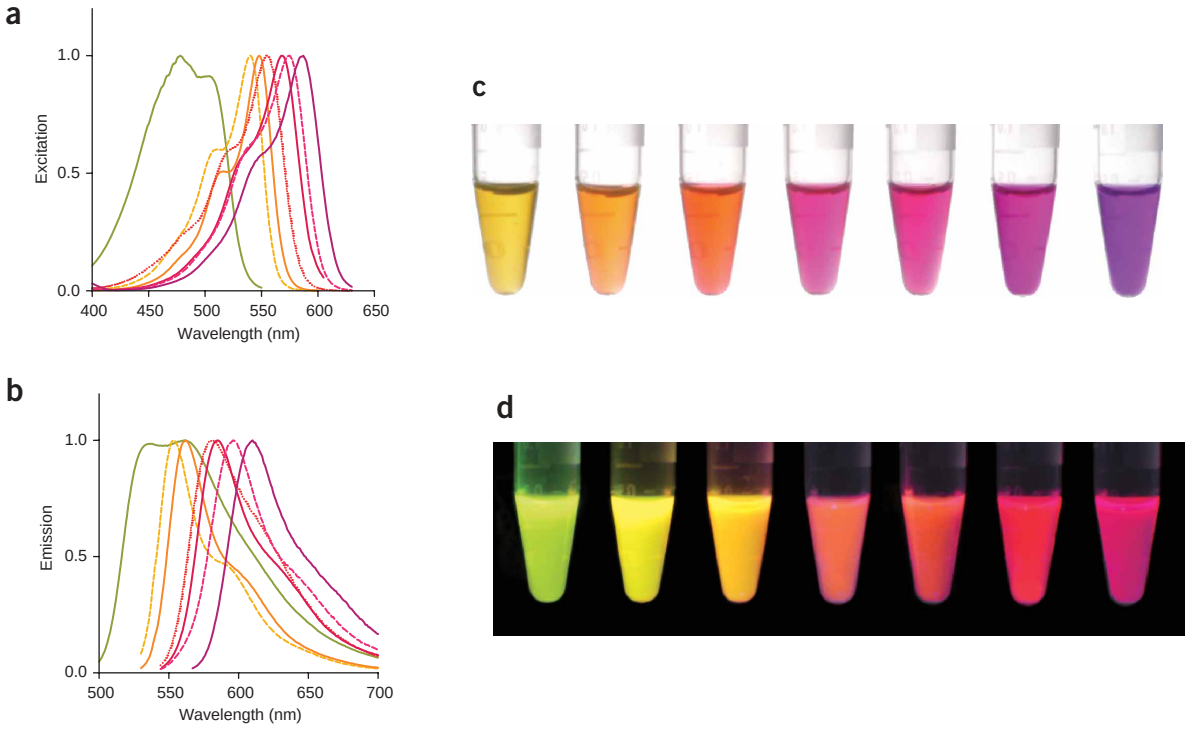

Figure 1 Excitation and emission spectra for new RFP variants. Spectra are normalized to the excitation and emission peak for each protein. (**a**,**b**) Excitation (**a**) and emission (**b**) curves are shown as solid or dashed lines for monomeric variants and as a dotted line for dTomato and tdTomato, with colors corresponding to the color of each variant. (**c**,**d**) Purified proteins (from left to right, mHoneydew, mBanana, mOrange, tdTomato, mTangerine, mStrawberry, and mCherry) are shown in visible light (**c**) and fluorescence (**d**). The fluorescence image is a composite of several images with excitation ranging from 480 nm to 560 nm.

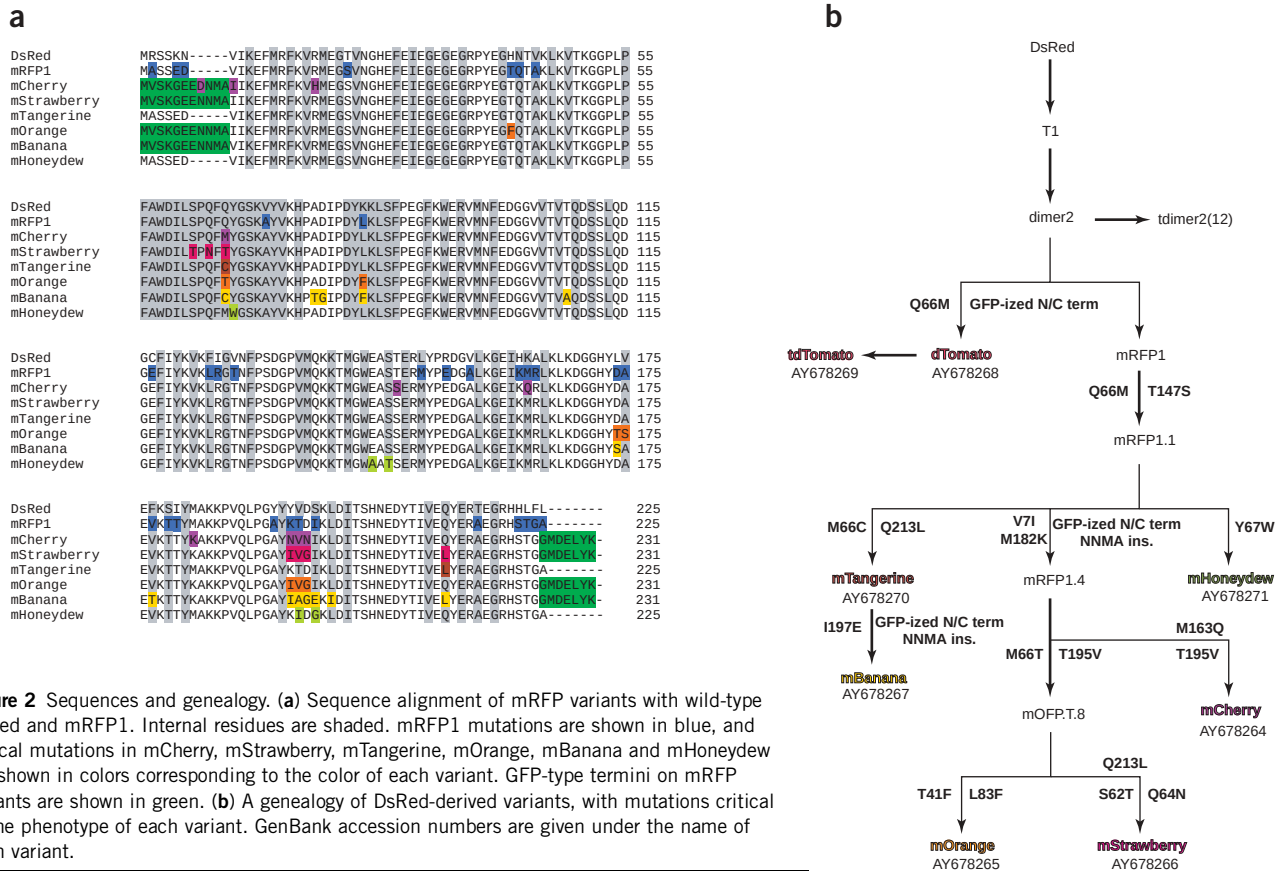

Figure 2 Sequences and genealogy. (**a**) Sequence alignment of mRFP variants with wild-type DsRed and mRFP1. Internal residues are shaded. mRFP1 mutations are shown in blue, and critical mutations in mCherry, mStrawberry, mTangerine, mOrange, mBanana and mHoneydew are shown in colors corresponding to the color of each variant. GFP-type termini on mRFP variants are shown in green. (**b**) A genealogy of DsRed-derived variants, with mutations critical to the phenotype of each variant. GenBank accession numbers are given under the name of each variant.

fused two copies of the gene to create a tandem dimer (td), as previously reported[7] (see Methods).

Many new fluorescent proteins with different colors have been discovered in diverse anthozoan species, but so far they all suffer from obligate tetramerization and would require efforts similar to the evolution of mRFP1 to produce widely useful fusion partners[10]. Because such monomerization is usually tedious and often unsuccessful, it might be more efficient to alter the excitation and emission wavelength of mRFP through directed evolution. Following the example of GFP engineering[11,12], we explored substitutions at Gln66 and Tyr67, homologous to Tyr66 and Ser65 in GFP (see **Supplementary Notes** online for details on the variants mHoneydew (Y67W) and mBanana (Q66C, I197E)).

Initial mutations of position 66 in mRFP1.1 indicated that the substitutions Q66S, Q66T, and Q66C all yielded proteins substantially blue-shifted with respect to mRFP1. This led us to the development of mTangerine, which contains the substitutions Q66C and Q213L with respect to mRFP1.1 (**Fig. 2**), with excitation and emission peaks at 568 and 585 nm (**Fig. 1**). Although mTangerine has a respectable extinction coefficient (38,000 $M^{-1}cm^{-1}$) and quantum yield (0.3), we quickly moved on to development of Gln66-substituted mutants of mRFP1.4, with its optimized N and C termini.

Six rounds of directed evolution of mRFP1.4 M66T produced the final orange fluorescent variant, mOrange, with excitation and emission peaks at 548 nm and 562 nm (**Table 1** and **Figs. 1** and **2**), similar to those of a tetrameric orange fluorescent protein from *Cerianthus* sp.[13] and a monomer evolved from a *Fulgia concinna* fluorescent protein[14]. mOrange has an extinction coefficient equivalent to that of mCherry, but a more than threefold higher quantum yield. Though mOrange is the brightest true monomer in the present series, it does exhibit substantial acid sensitivity, with a pKa of 6.5. However, the popular *A. victoria* GFP variant enhanced yellow fluorescent protein, with a pKa of 7.1 (ref. 15), has been used successfully as a qualitative fusion tag by many researchers. Additionally, from the initial mRFP1.4 M66T clone, through five rounds of directed evolution, we created a pH-stable orange-red variant, mStrawberry, which has the highest extinction coefficient (90,000 $M^{-1}cm^{-1}$) of the true monomers. Its wavelengths (excitation 574 nm, emission 596 nm) and quantum yield (0.29) are intermediate between those of mCherry and mOrange (**Table 1** and **Figs. 1** and **2**).

The high extinction coefficient and quantum yield of mOrange made it attractive as a potential fluorescence resonance energy transfer (FRET) acceptor for GFP variants. To test this possibility, we constructed a Zn^{2+} sensor with mOrange and the violet-excited GFP mutant T-Sapphire[16] and compared it to the same sensor containing cyan fluorescent protein (CFP) and the citrine[17] variety of YFP. T-Sapphire was chosen as the donor because it is optimally excited below 425 nm, where mOrange is negligibly excited. The domain that changes its conformation upon binding Zn^{2+} was modified from the original zif-268-derived version[18] by mutating the two Zn^{2+}-binding cysteines to histidine to eliminate any possibility of oxidation. The fusion of CFP and citrine respectively to the N and C termini of the modified Zn^{2+} finger displayed a 5.2-fold ratio change upon addition of Zn^{2+}, with an apparent K_d of ~200 μM. The corresponding mOrange-T-Sapphire combination yielded a sensor whose 562- to 514-nm emission ratio increased sixfold upon Zn^{2+}

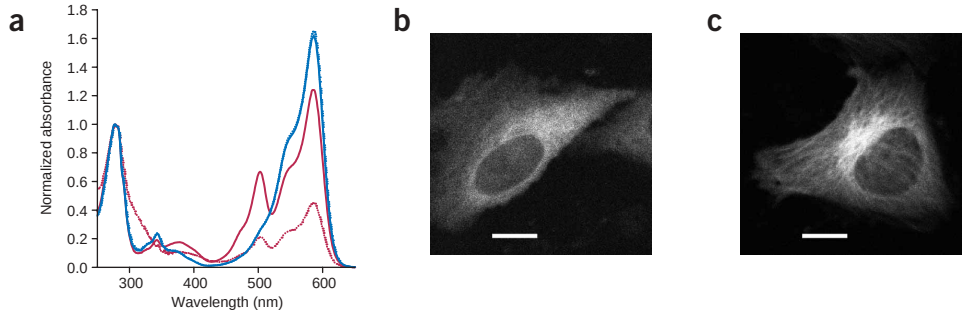

Figure 3 mCherry performance in fusion constructs. (**a**) mCherry is less sensitive than mRFP1 to the presence versus absence of an N-terminal fusion. mRFP1 and mCherry with N-terminal leader sequence containing a 6× His tag (derived from pRSET$_B$) or C-terminal tail with Myc-tag and 6× His tag (derived from pBAD-Myc-His-A (Invitrogen)) were purified on Ni-NTA agarose beads in parallel with extensive washes. Absorbance spectra were taken and normalized to the 280 nm peak for each. Absorbance curves for mRFP1 are plotted in red, and those from mCherry are plotted in blue. Solid lines correspond to N-terminal 6× His-tagged protein, and dotted lines correspond to C-terminal 6× His-tagged protein. Whereas mRFP1 exhibited greatly reduced expression and apparent extinction coefficient (approximately fourfold lower) when expressed with the C-terminal tag, mCherry produced nearly identical results with either N-terminal or C-terminal tags. (**b**,**c**) Expressed in HeLa cells by transient transfection, mRFP1-α-tubulin (**b**) fails to incorporate into microtubules, whereas mCherry-α-tubulin (**c**) is incorporated into microtubules, as has been shown before for *A. victoria*-derived fluorescent proteins[9]. The mRFP1-α-tubulin image (**b**) was brightened by a factor of 2.5 to enable comparison with the mCherry-α-tubulin image (**c**). Microtubules containing mCherry-α-tubulin display dynamic behavior as expected for functional microtubules (data not shown). Scale bars, 10 μm.

binding (**Supplementary Fig. 1** online). This demonstrates that mOrange and T-Sapphire make a good emission-ratiometric FRET pair with a dynamic range at least equaling CFP and YFP but at longer emission wavelengths.

What is the basis of the spectral shifts of these mRFP variants? The largest single effect is seen with substitutions at chromophore position 66, where substitution with serine, threonine or cysteine results in a substantial blue-shift. In the absence of compensating mutations, the Q66S/T/C variants of mRFP1 all exhibit emission around 580 nm at neutral pH, but become brighter and more blue-shifted at high pH. The blue-shifted (mOrange) species is stabilized by T41F and L83F mutations, whereas the red-shifted (mStrawberry) form is favored by S62T, Q64N and Q213L. In mBanana (see **Supplementary Notes** online), the I197E mutation may contribute a hydrogen bond between the glutamate side chain and phenolate oxygen in the chromophore, resulting in a further redistribution of electron density. Confirmation or more detailed explanations await high-resolution structural information.

An obvious application of the proliferation of fluorescent protein colors is to discriminate many cell types, transcriptional activities or fusion proteins. In the most general case, determination of the n independent concentrations of each of the fluorescent proteins requires spectral or lifetime unmixing of at least n measurements. Such unmixing techniques have been shown to discriminate fluorescent species having spectra even more closely overlapping than the current palette[19,20]. However, there is an important special case where each cell or nonoverlapping subcellular structure has been tagged with a different fluorescent protein. When a cell or voxel contains at most one fluorescent protein, how many measurements are required to decide its identity and concentration? To determine this, bacteria separately transfected with EGFP, citrine, mBanana, mOrange, mStrawberry or mCherry were mixed and analyzed by flow cytometry, with excitation at 514 nm and emission simultaneously measured through three bandpass filters, 540–560 nm, 564–606 nm and 595–635 nm. Transformation of the three signals to polar coordinates enabled easy discrimination of the six populations and the relative amounts of fluorescent protein per cell (**Supplementary Fig. 2** online). Thus three simple emission measurements are sufficient.

We compared the photostability of mRFP1 with that of its descendants and of EGFP (see Methods). To make fair comparisons among proteins with different extinction coefficients, overlaps with excitation filters and quantum yields, we normalized the bleach rates to an initial emission rate from each molecule of 1,000 photons/s. The resulting bleach curves (**Supplementary Fig. 3** online) varied greatly in absolute rate but were generally far from single exponentials. Most showed an initial fast phase in which over 50% of the initial emission was lost, followed by a lower-amplitude, much slower decay phase. This complexity makes it difficult to extract a meaningful single number for the quantum efficiency of photobleaching. Therefore, we believe a realistic figure of merit for typical cell biological experiments is the time for the emission to drop to 50% of its initial value. These values are listed in **Table 1**. By this criterion, the best performers are tdTomato and mCherry, which are both more than tenfold better than mRFP1 and nearly as good as EGFP.

Just as no one type of fruit in a grocery store supplants all others, so there is no single best fluorescent protein within the cornucopia derived from DsRed via mRFP1 and dimer2. The highest brightness (product of extinction coefficient, 138,000 $M^{-1}cm^{-1}$, and quantum yield, 0.69) is found in tdTomato, at the cost of doubling the molecular weight. A previous tandem dimer, t-HcRed1, was reported to have an extinction coefficient and quantum yield of 160,000 $M^{-1}cm^{-1}$ and 0.04 (ref. 21), corresponding to about 15-fold less brightness than that of tdTomato. Among the true monomers, mCherry offers the longest wavelengths, the highest photostability, the fastest maturation and excellent pH resistance. Its excitation and emission maxima are just 3 nm longer than those of mRFP1, for which it is the closest upgrade. Although mCherry's quantum efficiency is slightly lower (0.22 versus 0.25 for mRFP1), its higher extinction coefficient (due to near-complete maturation), tolerance of N-terminal fusions and photostability make mRFP1 obsolete. For applications such as dual-emission FRET in which the acceptor's quantum yield must be maximized, mOrange is the current favorite (e.g., **Supplementary Fig. 1** online), though its maturation time, pH sensitivity and photostability are currently far from optimal. Additional colors for multiwavelength tracking of distinct cells or

substructures are available from mStrawberry, mTangerine, mBanana and mHoneydew in descending order of wavelengths and brightness.

What other possibilities exist for the engineering of mRFP-derived proteins? Other desirable properties that exist in tetrameric fluorescent proteins and their relatives are reversible photoactivation[22], red-to-green photoconversion[23,24] and more extreme red-shifts[10,21,25]. One could also imagine the engineering of other more unconventional properties, such as phosphorescence or generation of singlet oxygen. Monomeric proteins with such properties would be quite valuable. Evolution of such proteins or recombination of the best features of the existing proteins will probably require even higher-throughput means to generate genetic diversity, coupled with new screens run in parallel for all requisite performance criteria.

METHODS

Mutagenesis and screening. mRFP1 and dimer2 (ref. 7) were used as the initial templates for construction of genetic libraries by a combination of saturation or partial saturation mutagenesis at particular residues and random mutagenesis of the whole gene. Random mutagenesis was performed by error-prone PCR as described[17] or by using the GeneMorph I or GeneMorph II kit (Stratagene). Mutations at specific residues were introduced as described[7], or by sequential QuikChange (Stratagene), or by QuikChange Multi (Stratagene) or by a ligation-based method (description follows). Briefly, oligonucleotide primers containing the degenerate codons of interest at their 5′ ends preceded by a *Sap*I restriction site were used to amplify the RFP in two separate PCR reactions using PfuTurbo polymerase (Stratagene). Each PCR fragment was cut with SapI (New England Biolabs) to produce a 3-base overhang compatible with the other digested fragment, and purified digested fragments were ligated with T4 DNA ligase (New England Biolabs). Full-length ligation product inserts were gel purified and digested with EcoRI/BamHI (New England Biolabs) and inserted into $pRSET_B$ or a modified pBAD vector (Invitrogen). For all library construction methods, chemically competent or electrocompetent *Escherichia coli* strain JM109(DE3) (for $pRSET_B$) or LMG194 (for pBAD)[26] were transformed and grown overnight on LB/agar (supplemented with 0.02% (wt/vol) L-arabinose (Fluka) for pBAD constructs) at 37 °C and maintained thereafter at 25 °C. Luria-Bertani (LB)/agar plates were manually screened as previously described[27]. JM109(DE3) colonies of interest were cultured overnight in 2 ml LB supplemented with ampicillin. LMG194 colonies of interest were cultured for 8 h in 2 ml minimal medium (RM) supplemented with ampicillin and 0.2% (wt/vol) D-glucose, and then culture volume was increased to 4 ml with LB/ampicillin. RFP expression was then induced by adding L-arabinose to a final concentration of 0.2% (wt/vol) and cultures were allowed to continue growing overnight. For both JM109(DE3) and LMG194, a fraction of the cell pellet was extracted with B-PER II (Pierce), and spectra were obtained using a Safire 96-well plate reader with monochromators (TECAN). DNA was purified from the remaining pellet by QIAprep spin column (Qiagen) and submitted for sequencing.

Construction of tandem dimer and FRET constructs. To construct tdTomato with a 12-residue linker (GHGTGSTGSGSS), dTomato was amplified in two separate PCR reactions, the first PCR retaining the 7-residue GFP-type N terminus (MVSKGEE) but deleting the 7-residue GFP-type C terminus and adding the first half of the 12-residue linker followed by a *Sap*I restriction site, and the second PCR adding the remaining half of the 12-residue linker followed by the sequence ASSEDNNMA before residue 7 of dTomato, and ending with the 7-residue GFP-type C terminus (GMDELYK). Agarose gel-purified PCR products were digested with *Sap*I, gel purified and ligated with T4 DNA ligase. The full-length ligation product was gel purified, digested with *Eco*RI/*Bam*HI and ligated into a modified pBAD vector. For FRET constructs, the original Zn^{2+} sensor[18] was modified such that the two Zn^{2+}-ligating cysteine residues were mutated to histidine. The modified Zn^{2+} finger domain, HERPYA**H**PVES**H**DRFSRSDELTR**H**IRI**H**TGQK (Zn^{2+} ligating residues in bold, mutated residues underlined), was inserted between CFP and citrine with *Sph*I and *Sac*I sites as linkers. PCR-amplified mOrange and T-Sapphire[16] were inserted into *Bam*HI/*Sph*I and *Eco*RI/*Sac*I sites, replacing CFP and citrine.

Protein production and characterization. RFPs were expressed from pBAD vectors in *E. coli* LMG194 by growing single colonies in 40 ml RM/ampicillin supplemented with 0.2% D-glucose for 8 h, adding 40 ml LB/ampicillin and L-arabinose to a final concentration of 0.2%, and incubating overnight at 37 °C. For maturation experiments, flasks were sealed with parafilm upon induction to restrict oxygen availability. All proteins were purified by Ni-NTA chromatography (Qiagen) and dialyzed into PBS. Biochemical and fluorescence characterization experiments were done as described[5]. For FRET measurements, purified Zn^{2+} sensor proteins were diluted in 10 mM MOPS, 100 mM KCl, pH 7.4 with either 1 mM EDTA or 1 mM $ZnCl_2$, and fluorescence emission spectra were collected with excitation near the peak donor excitation wavelength.

Cloning of tubulin chimeras, transfection and imaging. cDNAs were inserted following standard procedures into the *Hin*dIII and *Xho*I sites of pCDNA3.1 (Invitrogen), resulting in cDNAs encoding mRFP1-GGR-human-α-tubulin and mCherry-SGLRSRA-human-α-tubulin, both lacking the first methionine of tubulin. PCR-mediated cloning was verified by automated sequencing. HeLa cells were grown in 3-cm dishes with poly-D-lysine coated glass-bottoms (Matek) in DMEM supplemented with penicillin and streptomycin and 10% fetal calf serum. HeLa cells were transfected using Fugene (Invitrogen) and analyzed 2 d post-transfection. Imaging was done on a Biorad MRC1024 confocal system, controlled by Lasersharp2000 software. The stage was maintained at 37 °C using a lens heater (Bioptechs) and a 3-cm water-circulation-based dish heater. Acquisition was in one focal plane, using 568 nm excitation and collecting >585 nm emission.

Electrophoresis, in-gel fluorescence and western blot analysis. Transfected cells were lysed in 120 µl Laemmli Sample Buffer (50 mM Tris pH 6.8, 2% (wt/vol) SDS, 10% (vol/vol) glycerol, 5% (vol/vol) β-mercaptoethanol, 0.1% (wt/vol) bromophenol blue) and the lysates were sheared. Lysates were either left untreated (in-gel fluorescence assay) or heated for 10 min at 95 °C (western blot). We ran 15 µl of each sample on a 10–20% Novex Tris-Glycine gel (Invitrogen). Fluorescence was measured using 560/40 nm excitation and 620/20 nm emission filters. The gel with the denaturated samples was transferred to Immobilon (Millipore). The membranes were blocked in 2.5% (wt/vol) BSA and subsequently probed with primary antibody anti-α-tubulin (B512, Sigma) followed by goat-anti-mouse antibody conjugated to horseradish peroxidase (Calbiochem). Blots were washed extensively, and immunostained proteins were visualized using Western Lightning Chemiluminescence (Perkin Elmer).

FACS. A modified version of the protocol described[28] was used for FACS screening of large libraries of fluorescent protein mutants. Briefly, *E. coli* LMG194 was electroporated with a modified pBAD vector containing the gene library, and the transformed cells were grown in 30 ml RM supplemented with ampicillin and 0.2% (wt/vol) D-glucose. After 8 h, RFP expression was induced by adding L-arabinose to a final concentration of 0.2% (wt/vol). Cultures induced overnight were diluted 1:100 into Dulbecco's PBS supplemented with ampicillin before FACS sorting. Multiple rounds of cell sorting were done on a FACSDiva (BD Biosciences) in yield-mode for the first sort and purity- or single-cell mode for subsequent sorts of the same library. Sorted cells were grown overnight in 4 ml RM/amp with 0.2% (wt/vol) D-glucose and the resulting saturated culture was diluted 1:100 into 30 ml RM/Amp with 0.2% (wt/vol) D-glucose to start the next culture to be sorted. After three to four rounds of FACS sorting, the bacteria were plated onto LB/agar supplemented with 0.02% (wt/vol) L-arabinose and grown overnight, after which individual clones were screened manually as described above.

Photobleaching measurements. Aqueous droplets of purified protein in PBS were formed under mineral oil in a chamber on the fluorescence microscope stage. For reproducible results it proved essential to pre-extract the oil with aqueous buffer, which would remove any traces of autoxidized or acidic contaminants. The droplets were small enough (5–10 µm diameter) so that all the molecules would see the same incident intensity. The absolute excitation irradiance in photons/($cm^2 \times s \times nm$) as a function of wavelength was computed from the spectra of a xenon lamp, the transmission of the excitation filter, the reflectance of the dichroic mirror, the manufacturer-supplied absolute spectral sensitivity of a miniature integrating-sphere detector (SPD024 head and ILC1700 meter, International Light Corp.) and the measured detector current.

The predicted rate of initial photon emission per chromophore (before any photobleaching had occurred) was calculated from the excitation irradiance and absorbance spectrum (both as functions of wavelength), and the quantum yield. These rates varied from 180 s^{-1} for mHoneydew to 3,300 s^{-1} for mStrawberry. To normalize the observed photobleaching time courses to a common arbitrary standard of 1,000 emitted photons/s, the time axes were correspondingly scaled by factors of 0.18 to 3.3, assuming that emission and photobleach rates are both proportional to excitation intensity at intensities typical of microscopes with arc lamp sources, as is known to be the case for GFP[29].

Note: Supplementary information is available on the Nature Biotechnology website.

ACKNOWLEDGMENTS

All sequences have been deposited in GenBank, accession numbers AY678264 through AY678271. We thank Oliver Griesbeck for the kind donation of T-Sapphire, Coyt Jackson for FACS support, Brent Martin for α-tubulin cDNA, and Rene Meijer and Lei Wang for helpful discussion. Sequencing services were provided by the UCSD Cancer Center shared sequencing resource. N.C.S. is a Howard Hughes Medical Institute Predoctoral Fellow. Construction of tubulin fusions and mammalian cell imaging were conducted at the National Center for Microscopy and Imaging Research, which is supported by National Institutes of Health (NIH) grant RR04050 (to Mark H. Ellisman). This work was also supported by NIH and Department of Energy grants NS27177 and DE-FG-01ER63276.

COMPETING INTERESTS STATEMENT

The authors declare that they have no competing financial interests.

Received 7 July; accepted 5 October 2004
Published online at http://www.nature.com/naturebiotechnology/

1. Tsien, R.Y. The green fluorescent protein. *Annu. Rev. Biochem.* **67**, 509–544 (1998).
2. Zhang, J., Campbell, R.E., Ting, A.Y. & Tsien, R.Y. Creating new fluorescent probes for cell biology. *Nat. Rev. Mol. Cell Biol.* **3**, 906–918 (2002).
3. Lauf, U., Lopez, P. & Falk, M.M. Expression of fluorescently tagged connexins: a novel approach to rescue function of oligomeric DsRed-tagged proteins. *FEBS Lett.* **498**, 11–15 (2001).
4. Matz, M.V. *et al.* Fluorescent proteins from nonbioluminescent Anthozoa species. *Nat. Biotechnol.* **17**, 969–973 (1999).
5. Baird, G.S., Zacharias, D.A. & Tsien, R.Y. Biochemistry, mutagenesis, and oligomerization of DsRed, a red fluorescent protein from coral. *Proc. Natl. Acad. Sci. USA* **97**, 11984–11989 (2000).
6. Bevis, B.J. & Glick, B.S. Rapidly maturing variants of the *Discosoma* red fluorescent protein (DsRed). *Nat. Biotechnol.* **20**, 83–87 (2002).
7. Campbell, R.E. *et al.* A monomeric red fluorescent protein. *Proc. Natl. Acad. Sci. USA* **99**, 7877–7882 (2002).
8. Gross, L.A., Baird, G.S., Hoffman, R.C., Baldridge, K.K. & Tsien, R.Y. The structure of the chromophore within DsRed, a red fluorescent protein from coral. *Proc. Natl. Acad. Sci. USA* **97**, 11990–11995 (2000).
9. Rusan, N.M., Fagerstrom, C.J., Yvon, A.M. & Wadsworth, P. Cell cycle-dependent changes in microtubule dynamics in living cells expressing green fluorescent protein-alpha tubulin. *Mol. Biol. Cell* **12**, 971–980 (2001).
10. Verkhusha, V.V. & Lukyanov, K.A. The molecular properties and applications of Anthozoa fluorescent proteins and chromoproteins. *Nat. Biotechnol.* **22**, 289–296 (2004).
11. Heim, R., Cubitt, A.B. & Tsien, R.Y. Improved green fluorescence. *Nature* **373**, 663–664 (1995).
12. Heim, R., Prasher, D.C. & Tsien, R.Y. Wavelength mutations and posttranslational autoxidation of green fluorescent protein. *Proc. Natl. Acad. Sci. USA* **91**, 12501–12504 (1994).
13. Ip, D.T. *et al.* Crystallization and preliminary crystallographic analysis of a novel orange fluorescent protein from the Cnidaria tube anemone *Cerianthus* sp. *Acta Crystallogr. D Biol. Crystallogr.* **60**, 340–341 (2004).
14. Karasawa, S., Araki, T., Nagai, T., Mizuno, H. & Miyawaki, A. Cyan-emitting and orange-emitting fluorescent proteins as a donor/acceptor pair for fluorescence resonance energy transfer. *Biochem. J.* **381**, 307–312 (2004).
15. Llopis, J., McCaffery, J.M., Miyawaki, A., Farquhar, M.G. & Tsien, R.Y. Measurement of cytosolic, mitochondrial, and Golgi pH in single living cells with green fluorescent proteins. *Proc. Natl. Acad. Sci. USA* **95**, 6803–6808 (1998).
16. Zapata-Hommer, O. & Griesbeck, O. Efficiently folding and circularly permuted variants of the Sapphire mutant of GFP. *BMC Biotechnol.* **3**, 5 (2003). (http://www.biomedcentral.com/1472-6750/3/5).
17. Griesbeck, O., Baird, G.S., Campbell, R.E., Zacharias, D.A. & Tsien, R.Y. Reducing the environmental sensitivity of yellow fluorescent protein. Mechanism and applications. *J. Biol. Chem.* **276**, 29188–29194 (2001).
18. Miyawaki, A. & Tsien, R.Y. Monitoring protein conformations and interactions by fluorescence resonance energy transfer between mutants of green fluorescent protein. *Methods Enzymol.* **327**, 472–500 (2000).
19. Hadjantonakis, A.K., Dickinson, M.E., Fraser, S.E. & Papaioannou, V.E. Technicolour transgenics: imaging tools for functional genomics in the mouse. *Nat. Rev. Genet.* **4**, 613–625 (2003).
20. Farkas, D.L. *et al.* Non-invasive image acquisition and advanced processing in optical bioimaging. *Comput. Med. Imaging Graph.* **22**, 89–102 (1998).
21. Fradkov, A.F. *et al.* Far-red fluorescent tag for protein labelling. *Biochem. J.* **368**, 17–21 (2002).
22. Chudakov, D.M. *et al.* Kindling fluorescent proteins for precise *in vivo* photolabeling. *Nat. Biotechnol.* **21**, 191–194 (2003).
23. Mizuno, H. *et al.* Photo-induced peptide cleavage in the green-to-red conversion of a fluorescent protein. *Mol. Cell* **12**, 1051–1058 (2003).
24. Ando, R., Hama, H., Yamamoto-Hino, M., Mizuno, H. & Miyawaki, A. An optical marker based on the UV-induced green-to-red photoconversion of a fluorescent protein. *Proc. Natl. Acad. Sci. USA* **99**, 12651–12656 (2002).
25. Petersen, J. *et al.* The 2.0-A crystal structure of eqFP611, a far red fluorescent protein from the sea anemone *Entacmaea quadricolor*. *J. Biol. Chem.* **278**, 44626–44631 (2003).
26. Guzman, L.M., Belin, D., Carson, M.J. & Beckwith, J. Tight regulation, modulation, and high-level expression by vectors containing the arabinose PBAD promoter. *J. Bacteriol.* **177**, 4121–4130 (1995).
27. Baird, G.S., Zacharias, D.A. & Tsien, R.Y. Circular permutation and receptor insertion within green fluorescent proteins. *Proc. Natl. Acad. Sci. USA* **96**, 11241–11246 (1999).
28. Daugherty, P.S., Olsen, M.J., Iverson, B.L. & Georgiou, G. Development of an optimized expression system for the screening of antibody libraries displayed on the *Escherichia coli* surface. *Protein Eng.* **12**, 613–621 (1999).
29. Chiu, C.S., Kartalov, E., Unger, M., Quake, S. & Lester, H.A. Single-molecule measurements calibrate green fluorescent protein surface densities on transparent beads for use with 'knock-in' animals and other expression systems. *J. Neurosci. Methods* **105**, 55–63 (2001).
30. Ward, W.W. Biochemical and physical properties of GFP. in *Green Fluorescent Protein: Properties, Applications, and Protocols* (eds. Chalfie, M. & Kain, S.) 45–75 (Wiley, New York, 1998).